Electronic Supplementary Material (ESI) for Chemical Communications.

Tuning Molecular Rotor Dynamics by CO_2 Adsorption in Porous Materials

Silvia Bracco,[a] *Tetsuya Miyano,*[a,b] *Mattia Negroni,*[a] *Irene Bassanetti,*[a]
Luciano Marchiò,[c] *Piero Sozzani,*[a]* *Norimitsu Tohnai,*[b]*
Angiolina Comotti[a]*

a) Department of Materials Science, University of Milano Bicocca,
Via R. Cozzi 55, 20125 Milano, Italy

b) Department of Material and Life Science, Graduate School of Engineering,
Osaka University 2-1 Yamadaoka, Suita, Osaka 565-0871, Japan

and

c) Department of Chemistry, University of Parma,
Parco Area delle Scienze 17/a, 43124 Parma, Italy

Table of Contents

Figure S14-16. Crystal structure of compound **1** sealed at 20 bar under CO_2.

Figure S17. Close contacts between the CO_2 molecule and the anion and cation groups surrounding the cavity.

Figure S18. Molecular fragments, Hirshfeld surface, curvedness and shape index over the Hirshfeld surface of the anion in the crystal structure of CO_2-loaded compound **1**.

Figure S19. Molecular fragments, Hirshfeld surface, curvedness and shape index over the Hirshfeld surface of CO_2 in the crystal structure of CO_2-loaded compound **1**.

Figure S20. Molecular fragments, Hirshfeld surface, curvedness and shape index over the Hirshfeld surface of the cation in the crystal structure of CO_2-loaded compound **1**.

Figure S21. Center of mass of CO_2 molecules (red dots) resulting from GCMC simulation at a loading of 71 cm^3g^{-1}.

Figure S22. Center of mass of CO_2 molecules (red dots) resulting from GCMC simulation at a loading of 83 cm^3g^{-1}.

1. General methods

Synthesis of 4,4'-bis(sulfophenylethynyl)benzene BSPEB, 4,4'-bis(sulfophenylethynyl)-d_4-benzene d_4-BSPEB, the BSPEB/benzylamine and d_4-BSPEB/benzylamine compounds

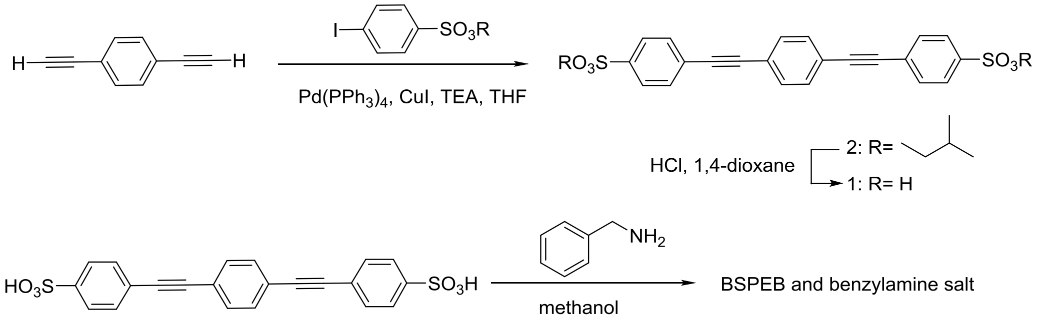

To a mixture of isobutyl-4-iodobenzenesulfonate (5.99 g, 17.6 mmol), Pd(PPh$_3$)$_4$ (0.924 g, 0.800 mmol), CuI (0.152 g, 0.800 mmol) and triethylamine (150 ml) deoxygenated by N$_2$ bubbling was added 1,4-diethynylbenzene (1.01 g, 8.00 mmol) dissolved in THF (8.0 ml), and the reaction mixture was stirred at room temperature for 24 h under N$_2$ atmosphere. After the solvent was removed in vacuo, the reaction mixture was washed with hexane. The product was purified by column chromatography (silica gel, CH$_2$Cl$_2$: hexane = 3:1) to yield protected-BSPEB (3.64 g, 6.61 mmol, 83%) as a white solid. Protected BSPEB, 1,4-dioxane, and 0.5M HCl were poured to pressure bottle and stirred at 100 ºC overnight. Protected BSPEB: ^{1}H NMR (400 MHz, CDCl$_3$): δ 7.91 (m, 4H), 7.70 (m, 4H), 7.56 (s, 4H), 3.84 (d, *J* = 6.4 Hz, 4H), 1.97 ppm, (m, 2H), 0.91 (d, *J* = 6.8 Hz, 12H). The mixture solvent was removed to yield BSPEB. BSPEB: ^{1}H NMR (400 MHz, DMSO-*d6*): δ 7.63 (d, *J* = 8.4 Hz, 4H), 7.62 (s, 4H), 7.53 (d, *J* = 8.4 Hz, 4H).

4,4'-bis(sulfophenylethynyl)-d_4-benzene (d_4-BSPEB) was synthesized starting from selectively deuterated d_4-1,4-diethynylbenzene. Protected d_4-BSPEB: ^{1}H NMR (400 MHz, CDCl$_3$): δ 7.91 (m, 4H), 7.70 (m, 4H), 3.85 (d, *J* = 6.4 Hz, 4H), 1.97 ppm, (m, 2H), 0.91 (d, *J* = 6.8 Hz, 12H). d_4-BSPEB: ^{1}H NMR (400 MHz, DMSO-*d6*): δ 7.63 (d, *J* = 8.8 Hz, 4H), 7.53 (d, *J* = 8.4 Hz, 4H).

The synthesis follows the procedure described in reference n. S1.

BSPEB and benzylamine were mixed in methanol in a 1:2 molar ratio. After the solution was removed in vacuo, the compound washed chloroform to yield pale yellow powder of the BSPEB/benzylamine supramolecular compound (Figure S1, Tables S1 and S2). IR (cm^{-1}): 3183wbr, 3078wbr, 2973wbr, 2924wbr, 2669w, 1600w, 1561m, 1466w, 1399w, 1239m, 1212s, 1172s, 1119s, 1122m, 1091w, 1036s, 1010s, 996m, 924m, 851m, 835s, 756m, 712vs, 698vs.

A similar procedure was followed for the preparation of the d_4-BSPEB/benzylamine supramolecular compound. IR (cm^{-1}): 3078wbr, 2983wbr, 2933w, 2869w, 2664w, 1619w, 1600w, 1526w, 1521w, 1463w, 1451w, 1398w, 1240m, 1208s, 1170s, 1124s, 1125s, 1127s, 1098m, 1035s, 1010s, 996m, 885m, 872s, 834s, 751m, 752m, 701vs.

Table S1. ^{1}H NMR (400 MHz) in DMSO of BSPEB/benzylamine adduct.

Chemical Shift Values	Proton Atoms	Integral Values	Multiplicity
4.05	He	4	s
7.38-7.48	Hd	10.33	m
7.55	Hb	3.96	d
7.63	Hc	3.87	s
7.65	Ha	4.03	d
8.12	Hf	5.86	sbr

Table S2. ^{1}H NMR (400 MHz) in DMSO of d_4-BSPEB/benzylamine adduct.

Chemical Shift Values	Proton Atoms	Integral Values	Multiplicity
4.05	He	4	s
7.38-7.47	Hd	9.92	m
7.54	Hb	4.06	d
7.65	Ha	4.16	d
8.12	Hf	5.34	sbr

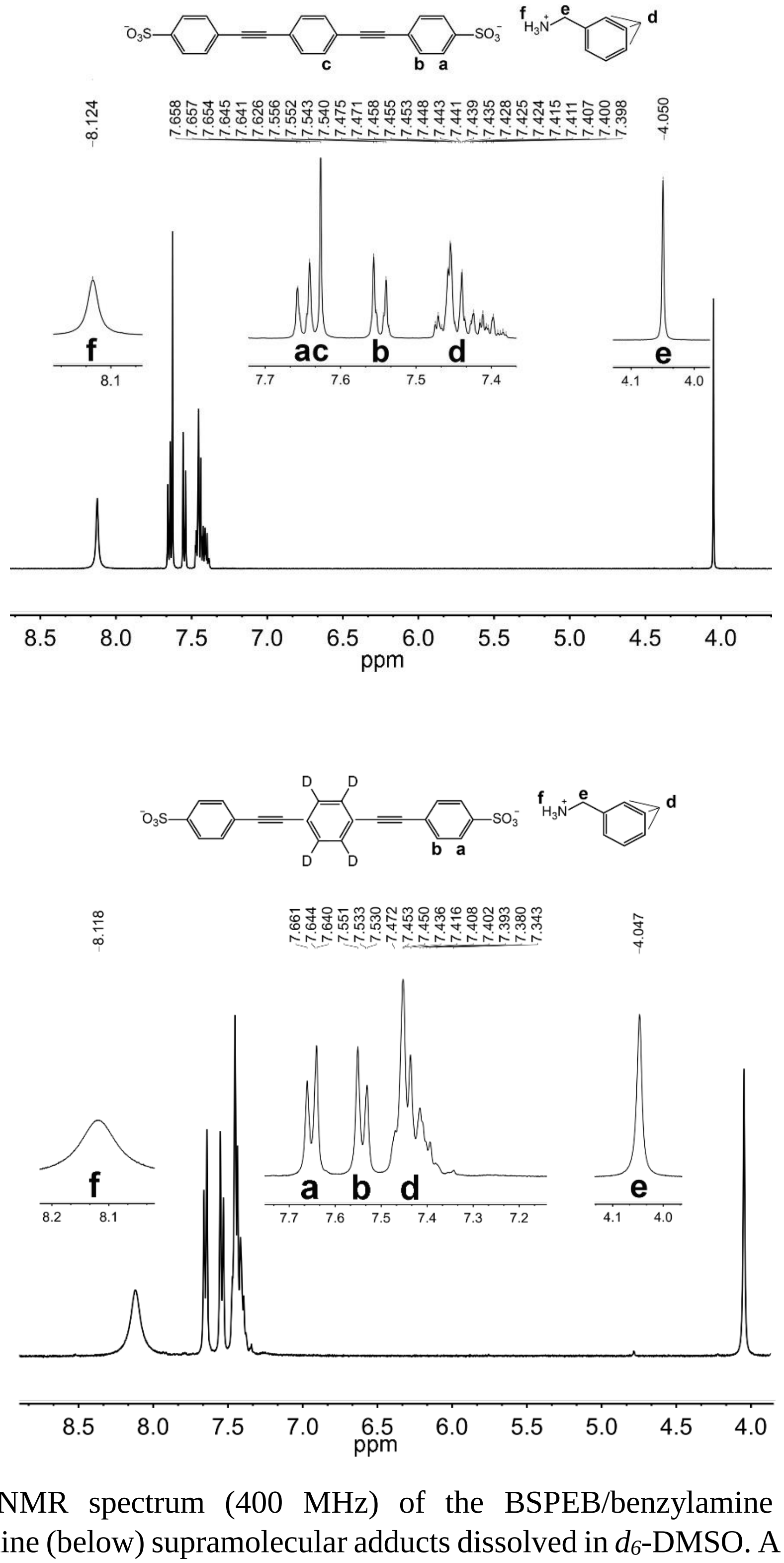

Figure S1. ^{1}H NMR spectrum (400 MHz) of the BSPEB/benzylamine (above) and d_4-BSPEB/benzylamine (below) supramolecular adducts dissolved in d_6-DMSO. A ratio of 2 between the BSPEB and benzylamine (and between d_4-BSPEB and benzylamine) was measured.

Preparation of single crystals

The BSPEB/benzylamine addcut was dissolved in methanol and then 1,4-dioxane was added to yield crystals of inclusion compound with 1,4-dioxane. The crystals were collected from the solution by filtration and used for various measurements.

In order to prepare single crystals of Form-A of the inclusion compound for single crystal X-ray diffraction measurement and analysis, the BSPEB/benzylamine adduct was dissolved in dry methanol and then dry 1,4-dioxane was added to the methanol. Slow evaporation of the solvent at room temperature under N_2 atmosphere gave suitable single crystals. On the other hand, slow evaporation of methanol and 1,4-dioxane under normal atmosphere gave crystals of Form-B. The single crystals of fully evacuated porous structure (porous compound **1**) were prepared by heat treatment of inclusion compound with 1,4-dioxane at 80 ºC in vacuum.

The same procedure was followed for the preparation of porous crystals of selectively deuterated compound d_4-**1**.

2. Experimental part

Thermogravimetric analysis measurements

Thermogravimetric (TG) analysis was performed on Rigaku Thermoplus TG8121 with N_2 gas flow (100 mL/min) from 30 to 300 ºC at a heating rate of 5 ºC min^{-1}.

^{1}H NMR measurements

^{1}H NMR spectra were measured on a JEOL spectrometer at 400 MHz.

Powder X-ray diffraction patterns

Powder X-ray diffraction (PXRD) patterns were collected by Rigaku Ultima IV using graphitemonochromatized CuKα radiation (λ = 1.54178 Å) at room temperature.

Gas adsorption measurements

The adsorption isotherms for CO_2 were carried out at 195 K and up to 760 mmHg on Micromeritics ASAP 2020 HD. Before all measurements, the sample was dried at 353 K for 1h. The BET surface area, as calculated by CO_2 adsorption isotherm at 195K, was of 332 and 291 m^2/g (Langmuir and BET surface area). CO_2 adsorption isotherms at 295 K and 273 K and up to 10 bar were performed on a Micromeritics ASAP 2050 instrument.

Solid State NMR experiments

The ^{13}C solid-state NMR spectra were run at 75.5 MHz, on a Bruker Avance 300 instrument operating at a static field of 7.04 T equipped with a 4 mm double resonance MAS probe. Ramped-amplitude cross polarization experiments were performed at a spinning speed of 15 kHz using a recycle delay of 6 s and a contact time of 0.05 and 2 ms. The 90° pulse used for proton was 2.9 μs. ^{13}C Single-pulse excitation (SPE) experiment was run using a recycle delay of 60 s.

^{13}C spin-lattice relaxation times were measured by applying the CP T_1 method developed by Torchia.[S2] Crystalline polyethylene was taken as an external reference at 32.8 ppm from TMS.

Phase-modulated Lee−Goldburg (PMLG) heteronuclear ^{1}H-^{13}C correlation (HETCOR) experiments coupled with fast magic angle spinning allowed the recording of the 2D spectra with a high resolution in both hydrogen and carbon dimensions. Narrow hydrogen resonances, with line widths on the order of 1−2 ppm, were obtained with homonuclear decoupling during t1; this resolution permits a sufficiently accurate determination of the proton species in the system. The 2D PMLG ^{1}H - ^{13}C HETCOR spectra were run with an LG period of 18.9 μs. The efficient transfer of magnetization to the carbon nuclei was performed by applying the RAMP-CP sequence. Quadrature detection in t1 was achieved by the time proportional phase increments method (TPPI). The carbon signals were acquired during t2 under proton decoupling by applying the two-pulse phase modulation scheme (TPPM).

The 2D ^{1}H-^{13}C HETCOR NMR experiments of porous compound d_4-**1** and compound **1** were conducted at 298 K under magic-angle spinning (MAS) conditions at 12.5 kHz with cross-polarization times of 0.05 ms, 0.5 ms and 2 ms. The 2D spectrum of compound **1** loaded with CO_2 at 2 bar was collected at 220 K at 8 kHz with a contact time of 5 ms.

Solid-state ^{2}H NMR spectroscopy experiments were performed on a Bruker 300 Avance spectrometer operating at a frequency of 46.07 MHz under a static magnetic field of 7.04 T, using a Bruker 4 mm wide-line probe. Fully relaxed spectra (15 s recycle delay) were acquired with the quadrupolar spin−echo pulse sequence, $(\pi/2)x - t_1 - (\pi/2)y - t_2$, with a π/2 pulse of 2.1 μs and a pulse spacing of $t_1 = t_2 = 30$ μs. Spectra obtained with a pulse spacing between 30 and 70 μs had the same line shapes. The stability and accuracy of the temperature controller (Bruker B-VT2000) were approximately 1 K. Theoretical simulation of ^{2}H NMR spectra for a two-site 180° jump model was performed by the program Express 1.0,[S3] with a quadrupolar coupling constant of 180 kHz and an asymmetry parameter of $\eta = 0.02$. The simulations are obtained for a log-Gaussian distribution of jump rates by superposition of 61 spectra for different jump rates. A single distribution width of $\sigma = 1.25$ was used. The attempt frequency of $2.4{*}10^{12}$ Hz and $4{*}10^{12}$ Hz were measured for the empty *d_4*-**1** and d_4-**1**/highCO_2 samples, respectively.

3. Crystallographic and physical data

Single crystal X-ray diffraction measurement and analysis of porous compounds

Diffraction data were collected on a two-dimensional X-ray detector (PILATUS 200K/R) equipped in Rigaku XtaLAB PRO diffractometer using thin multi-layer mirror monochromated Cu-Kα radiation (λ =1.54187 Å). The cell refinements were performed with a software CrysAlisPro 1.171.39.5a.[S4] A direct method of SHELXT [S5] was used for the structure solution of the crystals. All calculations were performed with the observed reflections [$I > 2\sigma(I)$] using the CrystalStructure crystallographic software package[S6], except for refinement which was performed by SHELXL.[S7] All non-hydrogen atoms were refined with anisotropic displacement parameters, and hydrogen atoms were placed in idealized positions and refined as rigid atoms with the relative isotropic displacement parameters.

For preliminary experiments, we used synchrotron radiation in SPring-8. Synchrotron radiation experiments were undertaken at BL38B1 in SPring-8 with approval of JASRI (proposal No. 2016A1610).

Table S3. X-ray crystallographic parameters for the crystals of inclusion compound with 1,4-dioxane, porous compound **1** and inclusion compound with 1,4-dioxane/water.

	Inclusion Compound with 1,4-dioxane (Form A)	Compound (**1**) Apo-A	Inclusion Compound with 1,4-dioxane/water Form-B
Formula	$(C_{22}H_{14}O_6S_2)_{0.5}$•$(C_7H_9N_1)$ • $(C_4H_4O_2)_{0.5}$	$(C_{22}H_{14}O_6S_2)_{0.5}$•$(C_7H_9N_1)$	$(C_{22}H_{14}O_6S_2)_{0.5}$•$(C_7H_9N_1)$ • $(C_4H_4O_2)_{0.5}$•(H_2O)
Fw	370.44	326.39	388.46
Crystal system	Monoclinic	Monoclinic	Triclinic
Space group	$P2_1/c$	$P2_1/c$	*P-1*
Temperature (K)	213	213	213
a (Å)	5.51851(12)	5.48472(15)	5.76413(11)
b (Å)	40.4605(8)	44.0584(14)	7.92695(17)
c (Å)	8.28955(19)	7.7312(3)	21.2914(5)
α	90	90	87.5578(18)
β	95.953(2)	92.467(2)	82.2517(18)
γ	90	90	84.7236(17)
V (Å^3)	1840.92(7)	1866.50(11)	959.43(4)
Z	4	4	2
reflections observed	10722	9700	9857
reflections unique	3747	3791	5770
R1 [I > 2.0σ(I)]	0.0567	0.0819	0.0496
Rw (all data)	0.1478	0.2240	0.1308
CCDC no.	1491087	1491086	1491236

Table S4. X-ray crystallographic parameters for the crystals of porous compound **1** at four distinct temperatures.

Temperature	**298 K**	**216 K**	**193 K**	**130 K**
a (Å)	5.4872(19)	5.4734(3)	5.4738(3)	5.4742(2)
b (Å)	44.133(9)	43.700(3)	43.726(3)	43.8531(18)
c (Å)	7.952(3)	7.8381(6)	7.8146(6)	7.7533(4)
β (Å)	92.97(3)	92.685(5)	92.677(6)	92.659(4)
Volume (Å^3)	1923.1(11)	1872.7(2)	1868.4(2)	1859.26(14)

Single crystal X-ray diffraction measurement and analysis of compounds with CO_2 sealed at 5 bar

The single-crystal data were collected on Bruker Smart 1000 and Bruker Smart APEXII area-detector diffractometers (Mo Kα; λ = 0.71073 Å). Datasets were collected at 298K. The cell parameters were refined from the observed setting angles and the detector positions of selected strong reflections. The intensities were integrated from several series of exposure frames that covered the sphere of the reciprocal space.

Table S5. X-ray crystallographic parameters for the crystals of compounds **1** with CO_2 loaded at 5 bar.

	Compounds **1** with CO_2 sealed at 5 bar
Formula	$(C_{22}H_{14}O_6S_2)_{0.5}$•$(C_7H_9N_1)$
Fw	326.39
Crystal system	Monoclinic
Space group	$P2_1/c$
Temperature (K)	298
a (Å)	5.557(17)
b (Å)	45.71(15)
c (Å)	7.88(3)
α	90
β	93.8(3)
γ	90
V (Å^3)	1999(2)
Z	4

Single crystal X-ray diffraction measurement and analysis of compounds with CO_2 sealed at 20 bar

Data collections of compound **1** under CO_2 pressure were performed at the X-ray diffraction beamline (XRD1) of the Elettra Synchrotron, Trieste (Italy).[S8] Crystals were inserted into a quartz capillary loaded with CO_2 at 20 bar and sealed. Datasets were collected at 220 K (nitrogen stream supplied by an Oxford Cryostream 700) through the rotating crystal method. Data were acquired using a monochromatic wavelength of 0.700 Å on a Pilatus 2M hybrid-pixel area detector. The diffraction data were indexed and integrated using XDS.[S9] Scaling have been done using CCP4-Aimless code.[S10,S11] The structures were solved by the dual space algorithm implemented in the SHELXT code.[S12] Fourier analysis and refinement were performed by the full-matrix least-squares methods based on F^2 implemented in SHELXL-2014. The assignment of the residual electron density in the cavities was performed as follows: the CO_2 molecules were modelled using the constraint of 1.16 Å C=O bond distance and linearity.

Table S6. Crystal data and structure refinement for compound **1** sealed with CO_2 at 20 bar.

Empirical formula	C38 H32 N2 O10 S2
Formula weight	740.77
Temperature/K	220(2)
Crystal system	Triclinic
Space group	P -1
a/ Å	5.6220(6)
b/ Å	7.3146(6) Å
c/ Å	22.8362(13) Å
α/°	85.588(6)
β/°	85.910(6)
γ/°	89.677(7)
Volume/Å^3	933.92(14)
Z	1
Density (calculated)	1.317 Mg/m^3
Absorption coefficient	0.195 mm^{-1}
F(000)	386
Crystal size/mm^3	0.28 x 0.11 x 0.04
Radiation	Synchrotron (0.7 Å)
2Θ range for data collection/°	5.30 to 51.89
Index ranges	-6<=h<=6, -9<=k<=9, -28<=l<=28
Reflections collected	8219
Independent reflections	3258 [R(int) = 0.0366]
Completeness to theta = 24.835°	86.2 %
Data / restraints / parameters	3258 / 3 / 209
Goodness-of-fit on F^2	2.600
Final R indices [I>2sigma(I)]	R1 = 0.2515, wR2 = 0.6528
R indices (all data)	R1 = 0.2578, wR2 = 0.6613
Largest diff. peak and hole	1.850 and -1.123 e.Å^{-3}
CCDC number	1544668

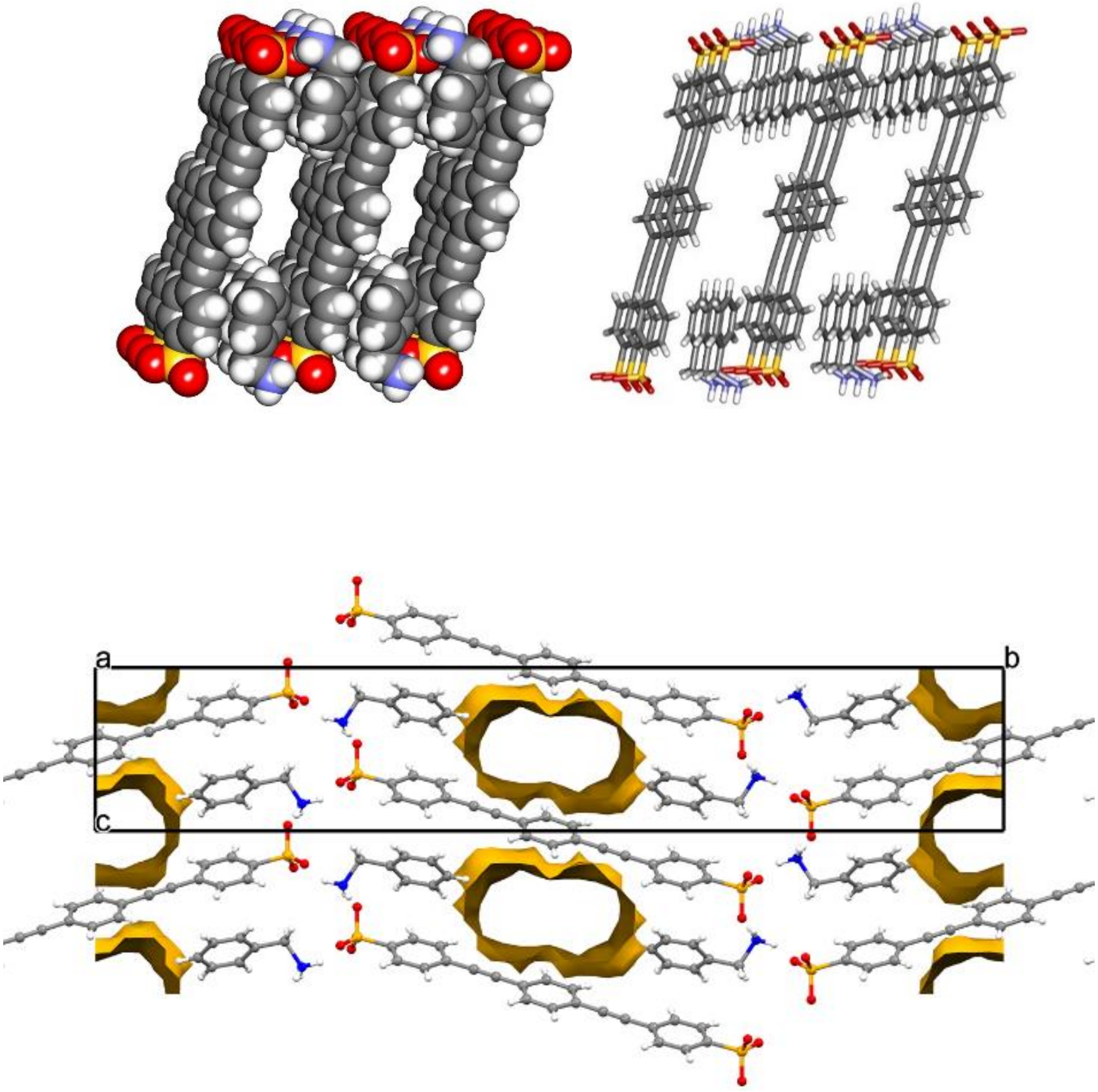

Figure S2. Above, crystal structure of porous compound **1**: CPK (left) and stick (right) representation. Below, crystal packing of porous compound **1**: the voids were obtained using a rolling sphere with a probe radius of 1.2 Å.

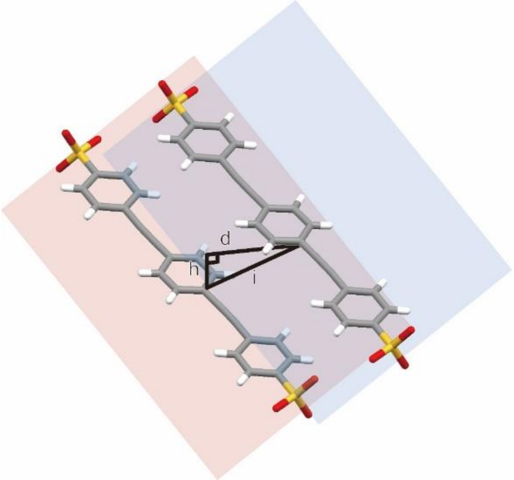

Figure S3. The distance between two adjacent p-phenylene rings (i) is 5.5 Å while the distance between two parallel adjacent planes (h) is 2.7 Å and horizontal distance (d) is 4.8 Å.

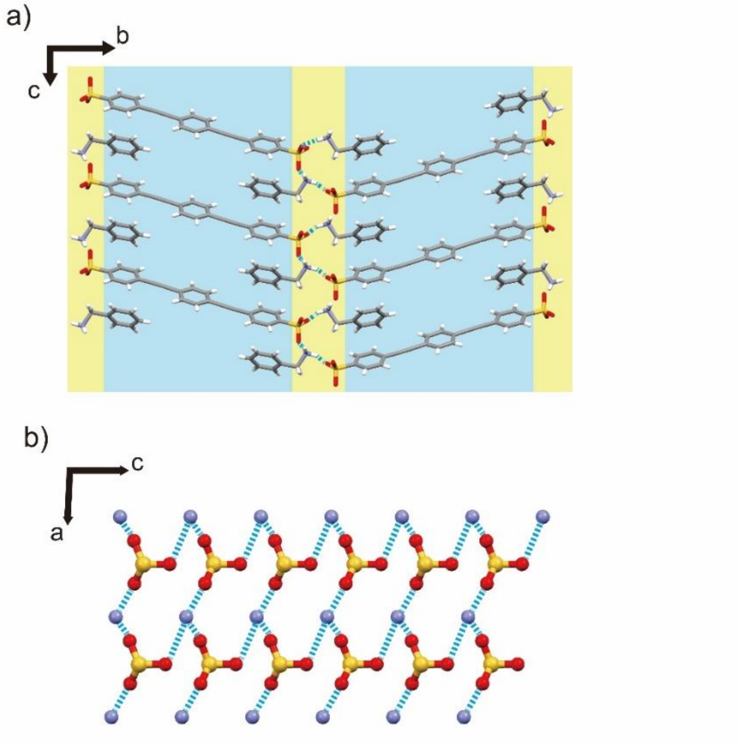

Figure S4. a) Representation of hydrophobic and polar double layers in the crystal structure of compound **1** as viewed along a axis. The yellow and blue areas represent respectively the polar and hydrophobic layers. b) Polar charge-assisted hydrogen bond network. The red, yellow and violet spheres represent respectively atoms of oxygen, sulfur and nitrogen. The hydrogen and carbon atoms were omitted.

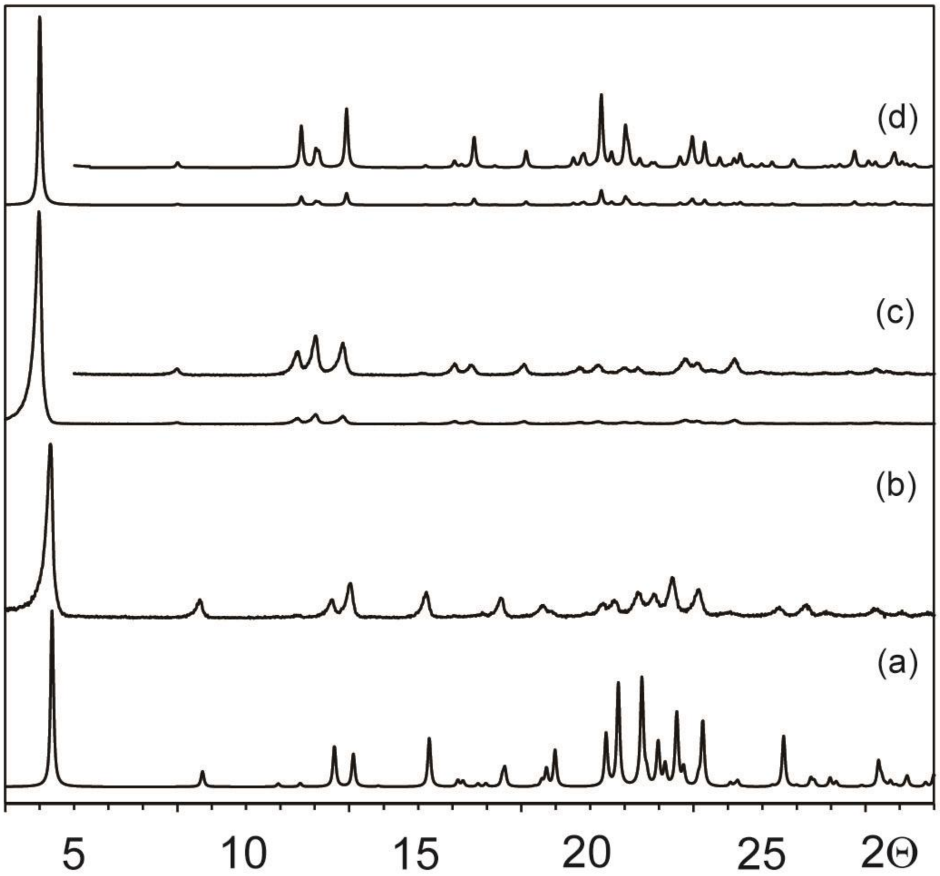

Figure S5. PXRD patterns: (a) simulated profile from the single crystal structure and (b) experimental profile of the inclusion compound BSPEB/1,4-dioxane; (c) experimental profile of the porous compound **1** prepared by the thermal treatment at 80°C under vacuum of the pristine inclusion compound and (d) simulated profile from the single crystal structure of the porous compound **1**.

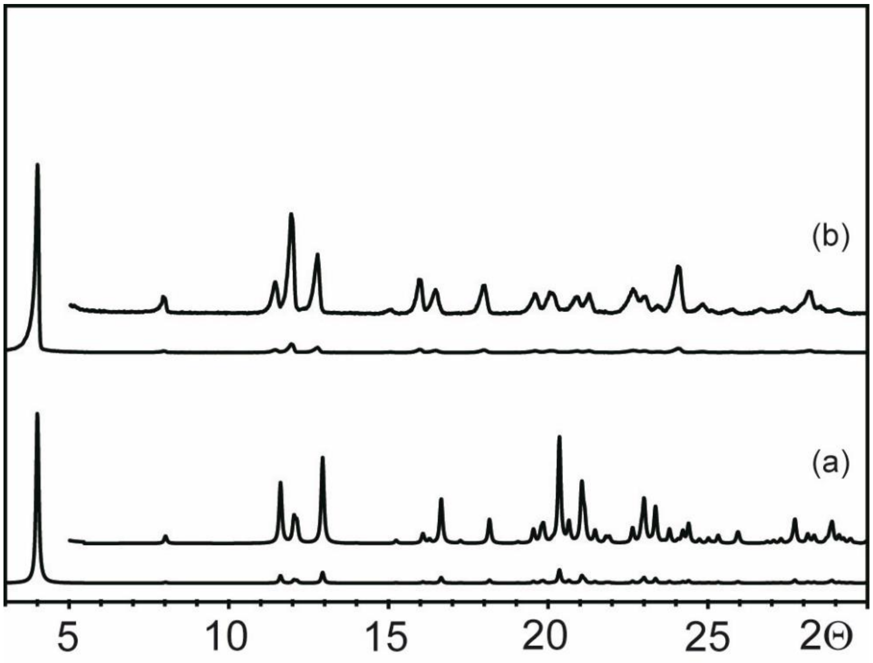

Figure S6. PXRD patterns: (a) simulated profile from the single crystal structure of the porous compound **1**; (b) experimental profile of porous compound *d₄*-**1** prepared by the thermal treatment at 80°C under vacuum of the pristine inclusion compound.

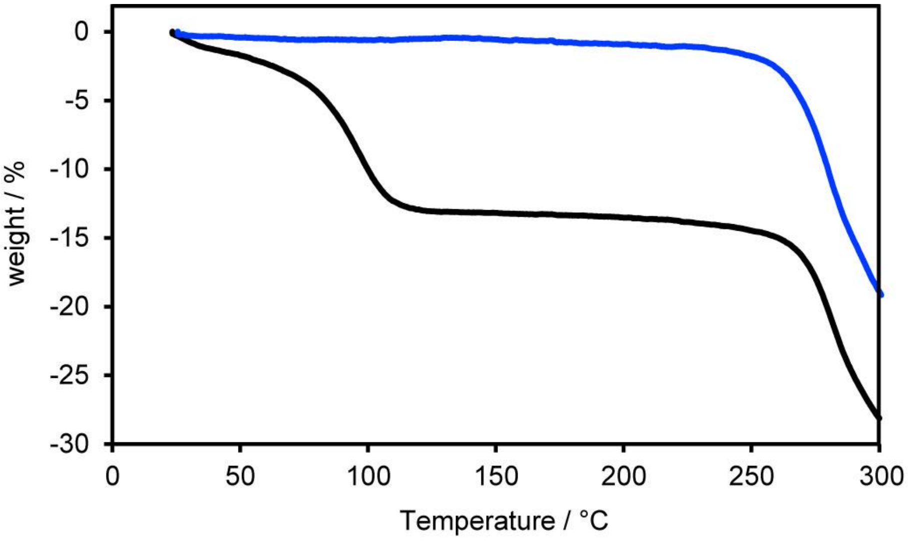

Figure S7. TGA runs of the porous crystal (blue line) and inclusion crystal BSPEB/1,4-dioxane (black line) at heating rate of 5°C/min under N_2 atmosphere. The weight loss at 100°C indicates the guest removal and the weight loss over 250°C is associated to the decomposition of the components.

Table S7. CO_2 loading and pressure as function of temperature of d$_4$-**1**/highCO2 (above) and d$_4$-**1**/midCO2 (below) samples used for ^{2}H NMR spectra.

d$_4$-**1**/highCO2			
T (K)	P (bar)	CO_2/rotor	mmol/g
298K	5.4	1.20	1.84
248K	1.2	1.66	2.49
212K	0.046	1.82	2.70
199K	0.046	1.82	2.70
191K	0.046	1.82	2.70
181K	0.046	1.82	2.70

d$_4$-**1**/midCO2			
T (K)	P (bar)	CO_2/rotor	mmol/g
298	3.3	0.95	1.45
242	0.544	1.58	2.40
210	0.027	1.70	2.61
196	0.027	1.70	2.61
179	0.027	1.70	2.61

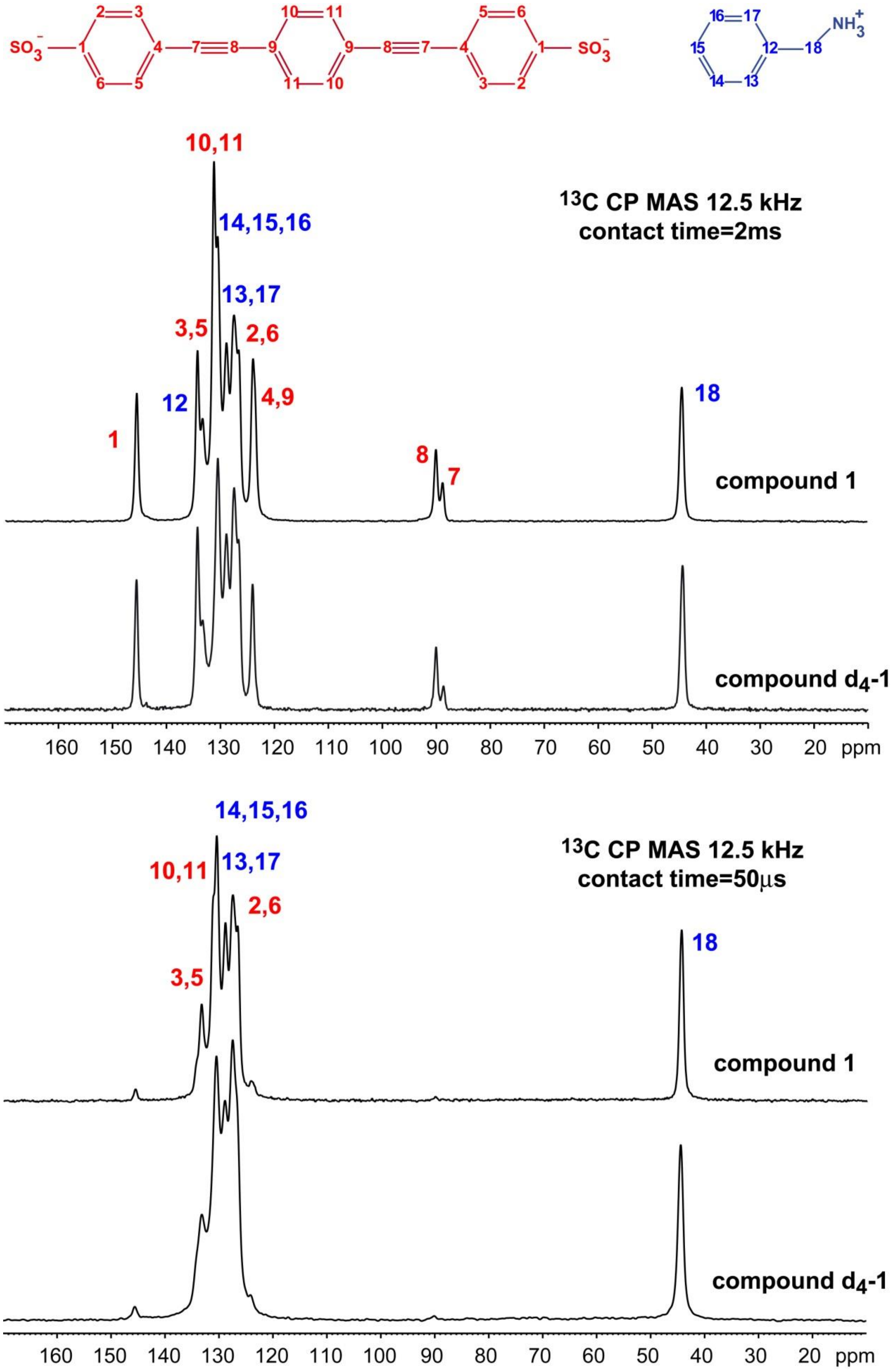

Figure S8. ^{13}C CP MAS NMR spectra of porous compounds **1** and *d*$_4$-**1** with contact times of 50 μs (below) and 2 ms (above).

Table S8. ^{13}C chemical shift of porous compounds **1** and d$_4$-**1**.

	Compound 1	**Compound *d*$_4$-1**
C atoms	δ/ppm	δ/ppm
1	145.63	145.58
2	126.71/127.58	126.59/127.31
3	133.42	133.38
4	124.04	123.93
5	133.42	133.38
6	126.71/127.58	126.59/127.31
7	88.87	88.70
8	90.10	90.05
9	124.04	123.45
10/11	131.29	130.79
12	134.35	134.23
13	128.98	128.84
14	130.62	130.79
15	130.62	130.79
16	130.62	130.79
17	128.98	128.84
18	44.47	44.27

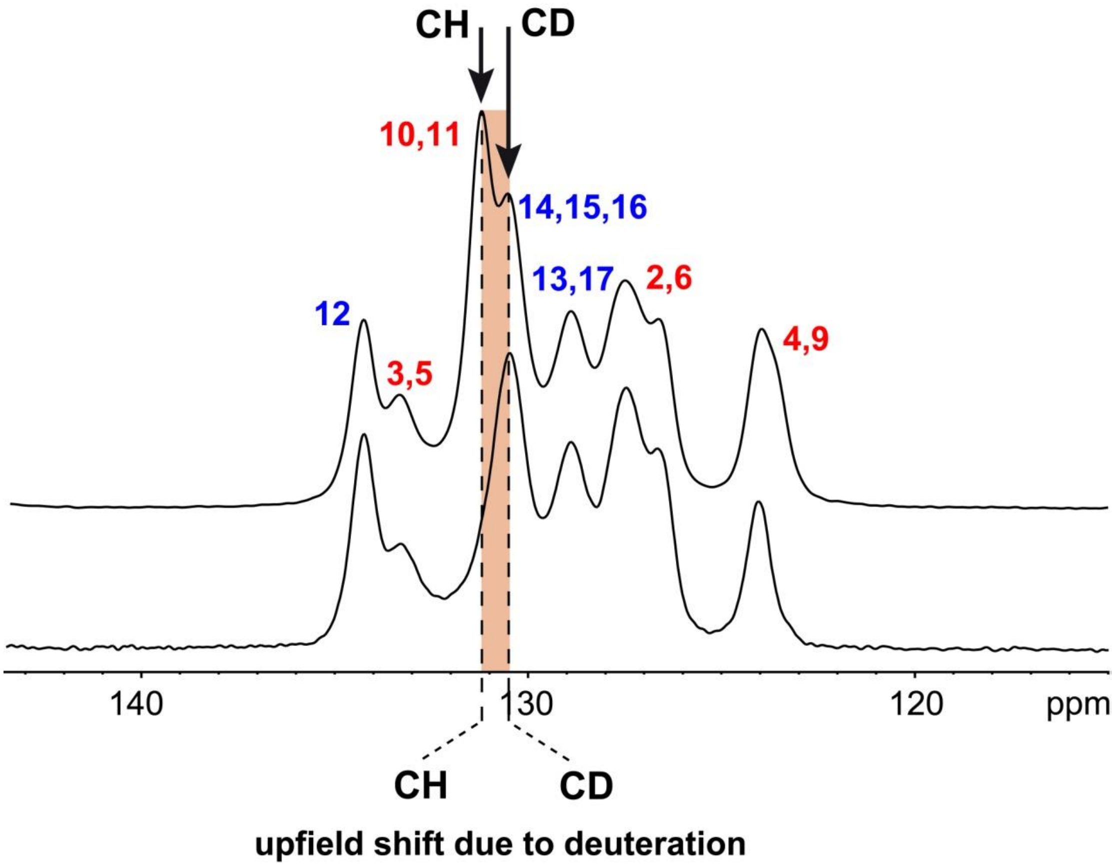

Figure S9. ^{13}C CP MAS NMR spectra of porous compounds **1** and *d_4*-**1**.

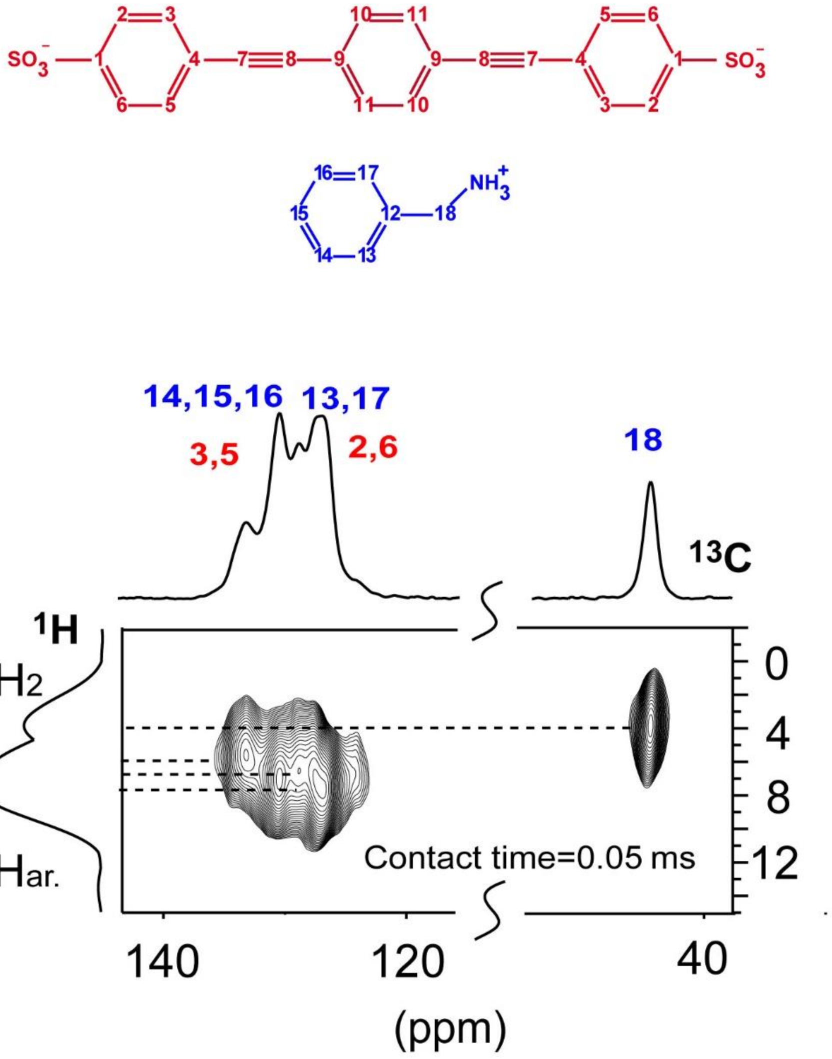

Figure S10. 2D ^{1}H-^{13}C HETCOR NMR spectrum of porous compounds d_4-**1** with short contact time (0.05 ms), selectively highlighting the cross-peaks of CH groups.

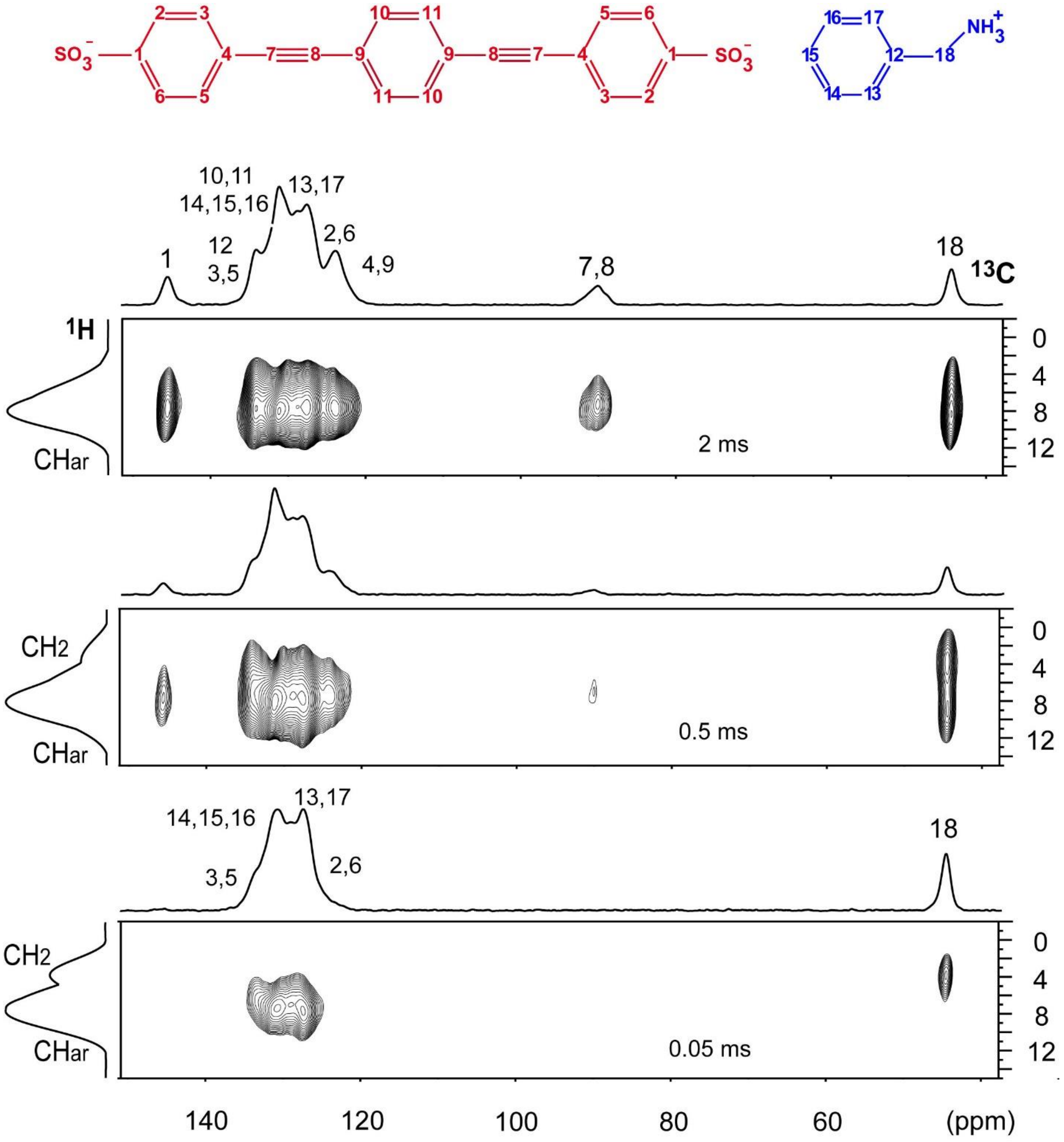

Figure S11. 2D ^{1}H-^{13}C HETCOR NMR spectrum of porous compounds **1** with different contact times (0.05 ms, 0.5 ms and 2 ms).

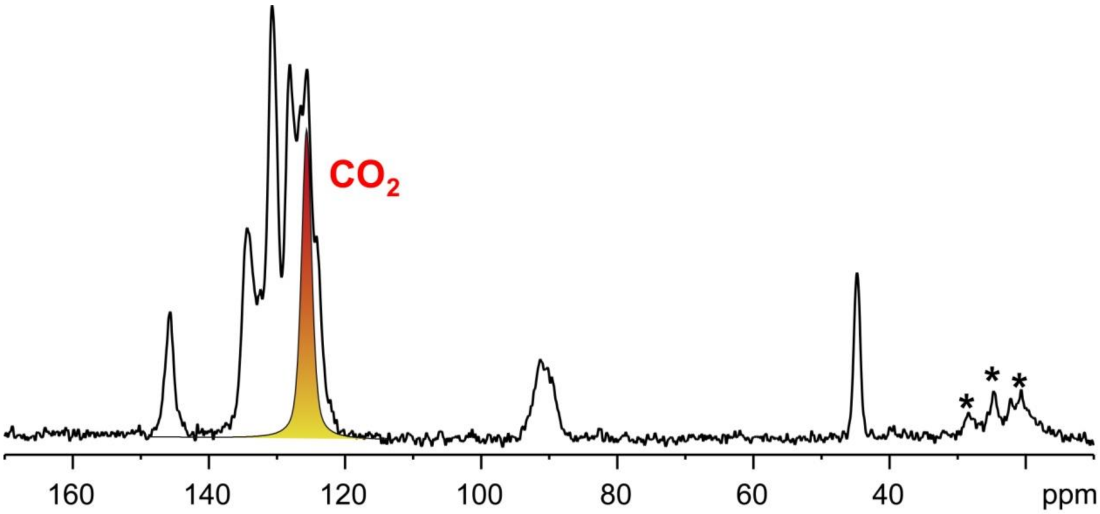

Figure S12. ^{13}C CP MAS NMR spectrum of CO_2-loaded compound **1** at 220 K performed with a contact time of 5 ms at 8 kHz spinning speed.

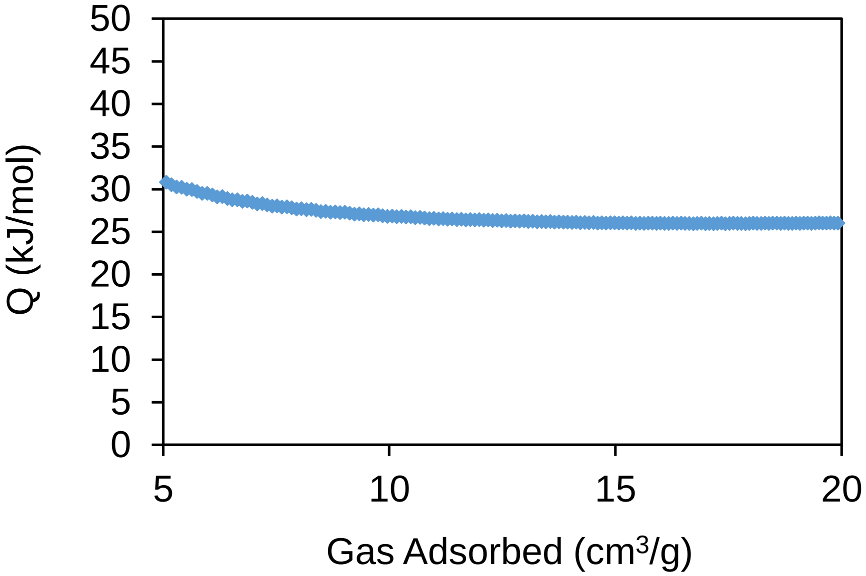

Figure S13. Isosteric heat of adsorption of CO_2 as calculated by Clausius-Clapeyron equation from CO_2 isotherms at 298 K and 273 K.

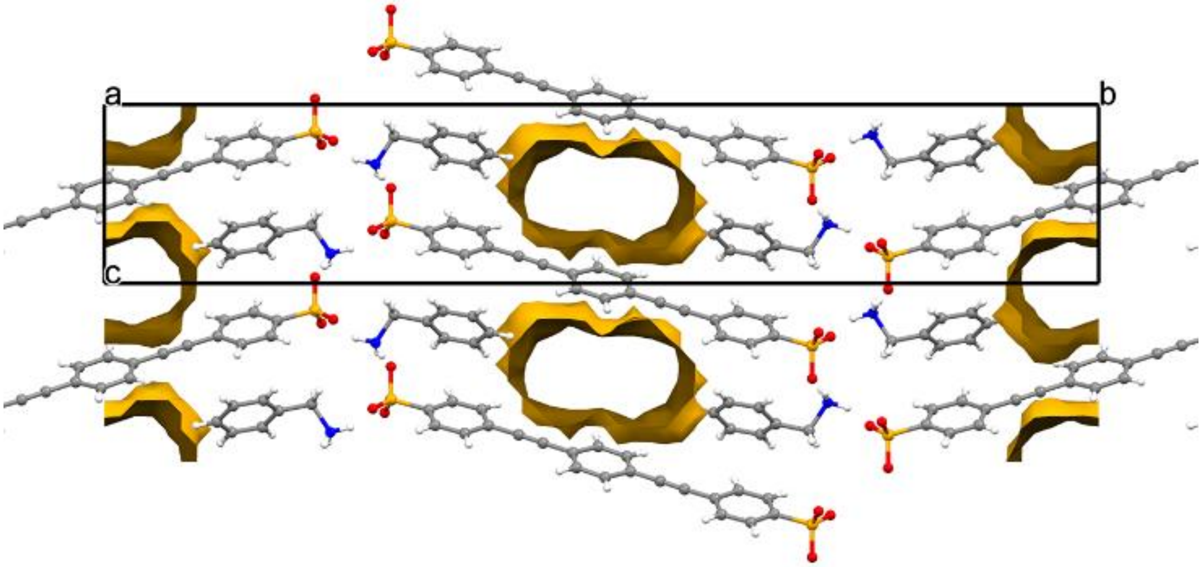

Figure S14. Crystal packing of compound **1** sealed at 20 bar under CO_2: the voids are described by a rolling a sphere with a probe radius of 1.2 Å.

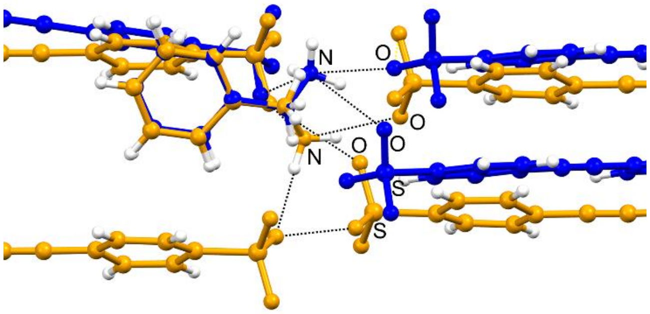

Figure S15. Charged-assisted hydrogen bonds between the benzylamonium cations and the sulphonate groups in compound **1** (blue) and compound **1** sealed at 20 bar under CO_2 (orange). The two structures were overlaid by minimizing the RMS of the two benzyl groups.

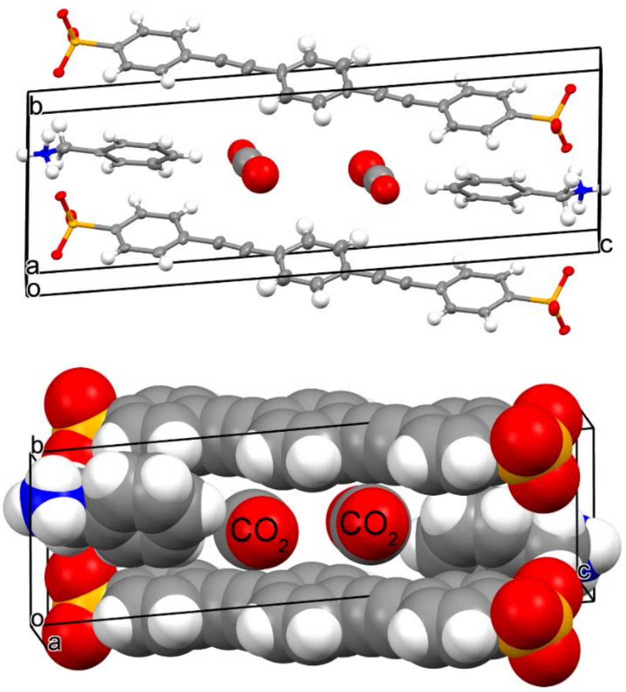

Figure S16. Above, unit cell content of porous compound **1** sealed at 20 bar under CO_2 depicted using thermal ellipsoids (30% probability level). Below, unit cell in spacefill representation.

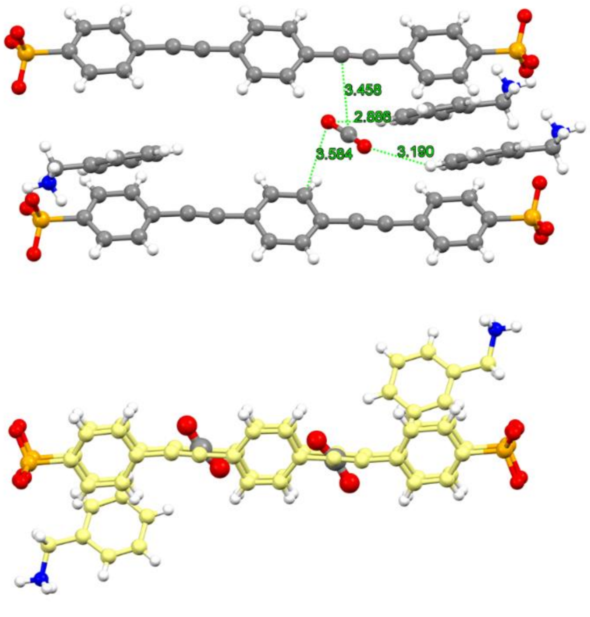

Figure S17. Close contacts between the CO_2 molecule and the anion and cation groups surrounding the cavity, distances are reported in Å. The CO_2 carbon atom is positioned between two alkyne carbon atoms. Moreover, one of the oxygen atoms is pointing toward a CH group of the cation, whereas the second oxygen atom is approximately superimposed on the CH fragment of the central phenyl ring.

Hirshfeld Surface Analysis.

The Hirshfeld surface (HS) properties were investigated to gain a description of the interactions occurring between the host moieties and CO_2. The HS defines the volume of space in a crystal in which the sum of the electron density of the spherical atoms for the molecule (promolecule) exceeds that for the crystal (procrystal).[S15] The HS surface and its properties were calculated using the CrystalExplorer 3.1 program.[S16]

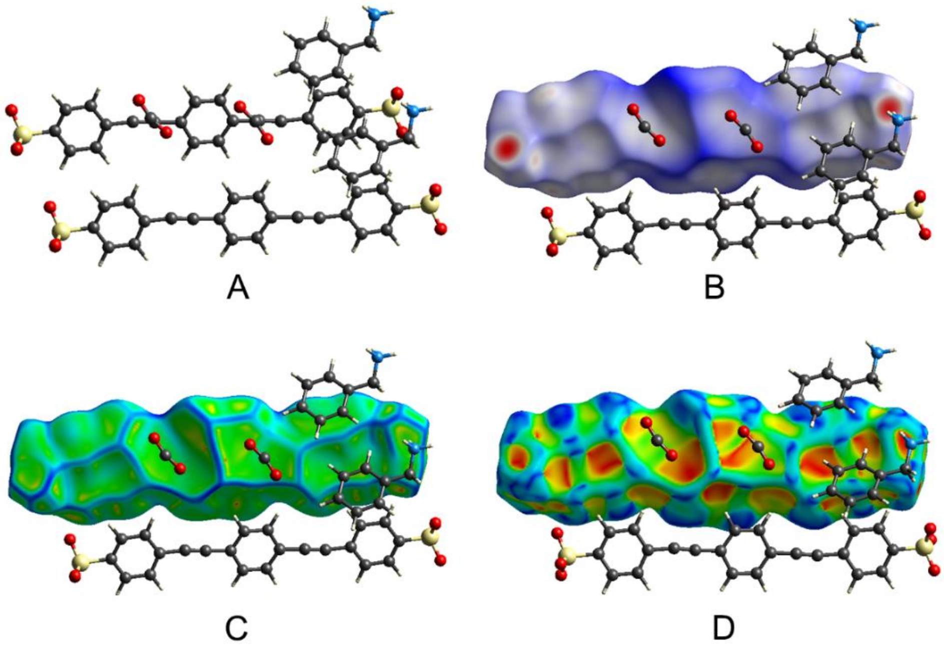

Figure S18. Molecular fragments (A) and Hirshfeld surface (B) of the anion.[S13,S14] Curvedness (C) and Shape index (D) reported over the Hirshfeld surface. Note the presence of two pockets on the central portion of the anion surface indicating a complementary match for the CO_2 fragment, compare D with Figure S19E below.

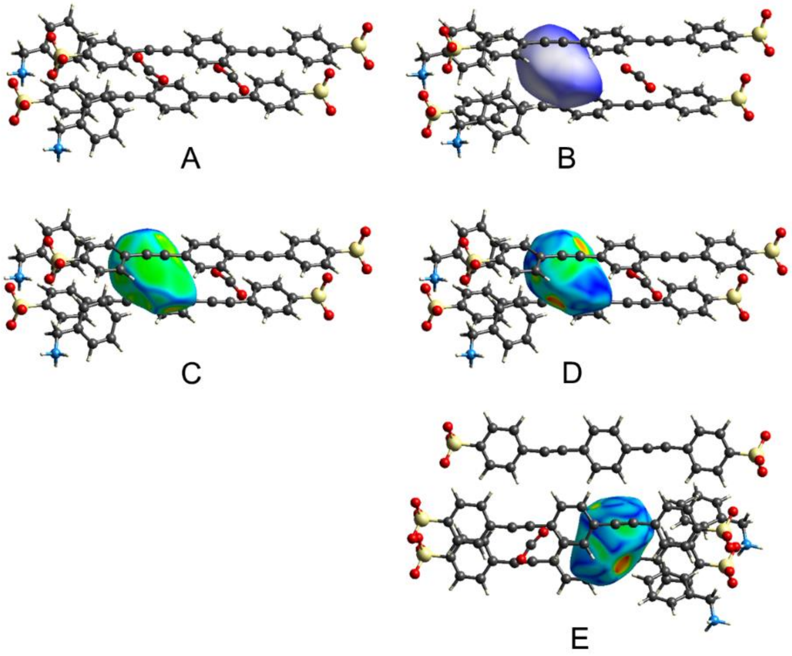

Figure S19. Molecular fragments (A) and Hirshfeld surface of the CO_2 (B). Curvedness (C) and shape index (D) reported over the Hirshfeld surface. On the shape index diagram (D and E) note the presence of regions indicating a complementary match with one cationic CH fragment, one CH of the central phenyl ring and the alkyne-phenyl framework, compare E with Figure S18D above.

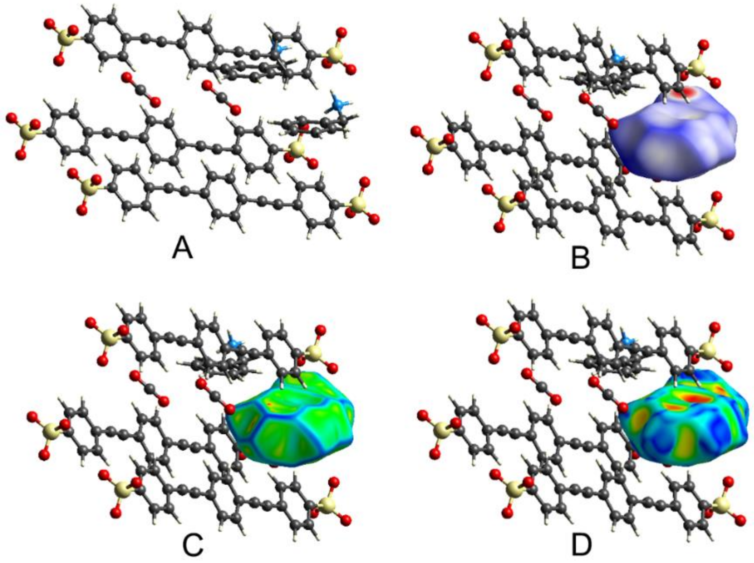

Figure S20. Molecular fragments (A) and Hirshfeld surface of the cation (B). Curvedness (C) and shape index (D) reported over the Hirshfeld surface. On the shape index diagram (D) note the presence of a two region indicating the complementary match with one of the CO_2 oxygen atom.

Grand Canonical Monte Carlo Simulations

Single component Grand Canonical Monte Carlo GCMC simulations were performed to calculate adsorbed amounts of CO_2. For GCMC simulations, a supercell of 4 × 3 × 1 crystallographic unit cells was used. The crystallographic cell, reduced to P_1 symmetry, was used as simulation box, using periodic boundary conditions to produce a homogeneous solid. COMPASS (v 2.8) force field was used. The cutoff distance for truncation of the intermolecular interactions was set to 15.5 Å.

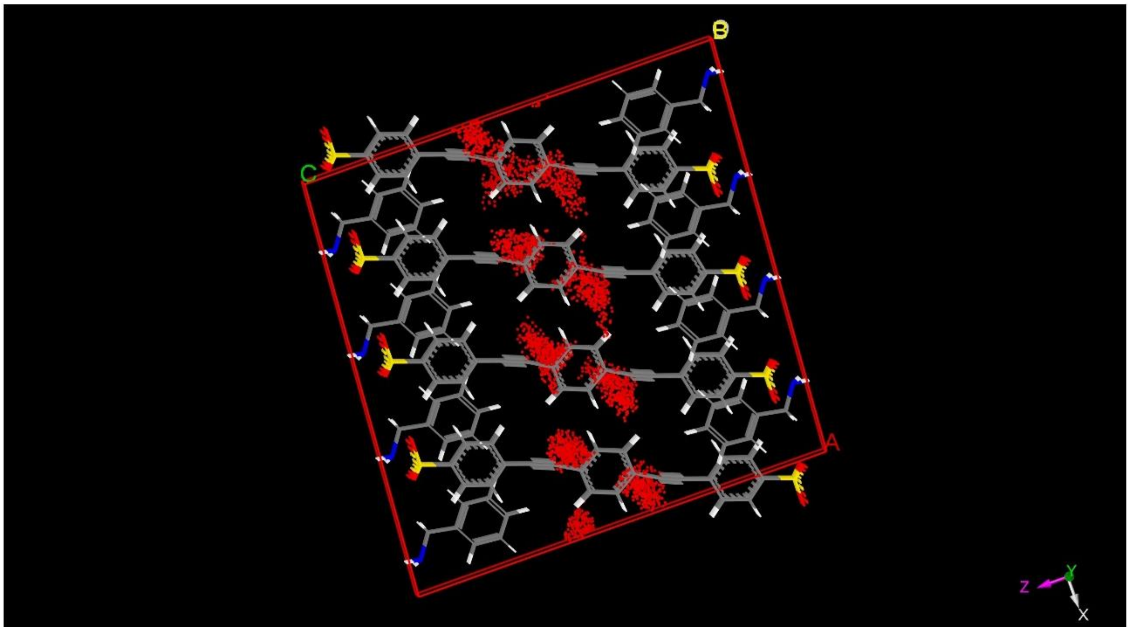

Figure S21. Center of mass of CO_2 molecules (red dots) resulting from GCMC simulation at a loading of 71 cm^3g^{-1}.

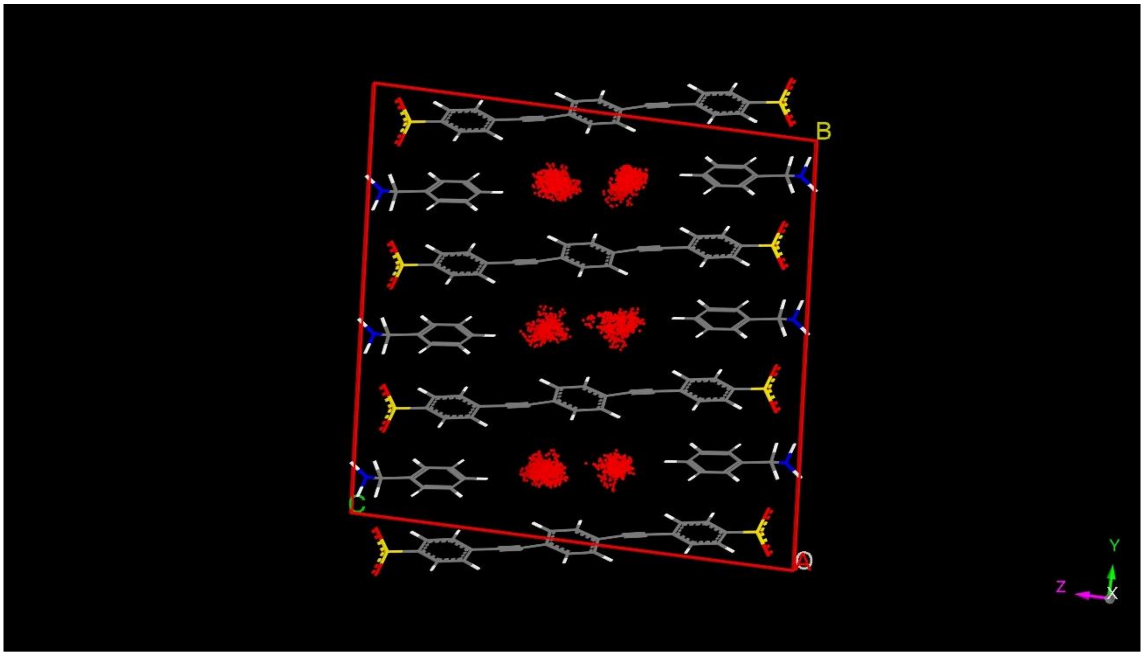

Figure S22. Center of mass of CO_2 molecules (red dots) resulting from GCMC simulation at a loading of 83 cm^3g^{-1}.

References

S1. Comotti, A.; Bracco, S.; Yamamoto, A.; Beretta, M.; Hirukawa, T.; Tohnai, N.; Miyata, M.; Sozzani, P. *J. Am. Chem. Soc.* **2014**, *136*, 618-621.

S2. Torchia, D. A. *J. Magn. Reson.* **1978**, *30*, 613-616.

S3. Vold, R. L.; Hoatson, G. L. *J. Magn. Reson.* **2009**, *198*, 57−72.

S4. Rigaku Oxford Diffraction (2015), Software CrysAlisPro 1.171.39.5a Rigaku Corporation, Tokyo, Japan

S5. Sheldrick, G. M. *Acta Cryst.* **2014**, *A70*, C1437.

S6. Rigaku (2015). CrystalStructure. Versions 4.2. Rigaku Corporation, Tokyo, Japan.

S7. Sheldrick, G.M. *Acta Cryst.* **2008**, *A64*, 112-122.

S8. Lausi, A.; Polentarutti, M.; Onesti, S.; Plaisier, J. R.; Busetto, E.; Bais, G.; Barba, L.; Cassetta, A.; Campi, G.; Lamba, D.; Pifferi, A.; Mande, S. C.; Sarma, D. D.; Sharma, S. M.; Paolucci, G. *Eur. Phys. J. Plus.* **2015**, *130*, 1-8.

S9. Kabsch, W. *Acta Crystal.* **2010**, *D66*, 125-132.

S10. Winn, M. D.; Ballard, C. C.; Cowtan, K. D.; Dodson, E. J.; Emsley, P.; Evans, P. R.; Keegan, R. M.; Krissinel, E. B.; Leslie, A. G. W.; McCoy, A.; McNicholas, S. J.; Murshudov, G. N.; Pannu, N. S.; Potterton, E. A.; Powell, H. R.; Read, R. J.; Vagin, A.; Wilson, K. S. *Acta Cryst.* **2011**, *D67*, 235-242.

S11. Evans, P. R.; Murshudov G. N. *Acta Cryst.* **2013**, *69*, 1204-1214

S12. Sheldrick, G. M. *Acta Cryst.* **2015**, *C71*, 3-8.

S13. McKinnon, J. J.; Jayatilaka, D.; Spackman, M. A. *Chem Commun.* **2007**,3814-3816.

S14. Spackman, M. A.; Jayatilaka, D. *Cryst. Eng. Comm.* **2009**, *11*, 19-32.

S15. (a) Spackman, M. A.; Jayatilaka, D. *Cryst. Eng. Comm.* **2009**, *11*, 19−32. (b) McKinnon, J. J.; Jayatilaka, D.; Spackman, M. A. *Chem. Commun*. **2007**, 3814−3816.

S16. Wolff, S. K.; Grimwood, D. J.; McKinnon, J. J.; Turner, M. J.; Jayatilaka, D.; Spackman, M. A. CrystalExplorer, Version 3.1; University of Western Australia: Perth, 2012.